J Mater Sci (2014) 49:4522–4529
DOI 10.1007/s10853-014-8152-0

Effects of multi-walled carbon nanotube (MWCNT) dispersion and compatibilizer on the electrical and rheological properties of polycarbonate/poly(acrylonitrile–butadiene–styrene)/MWCNT composites

In-Soo Han · Yun Kyun Lee · Heon Sang Lee · Ho Gyu Yoon · Woo Nyon Kim

Received: 30 December 2013 / Accepted: 7 March 2014 / Published online: 25 March 2014

Abstract In this study, the effects of multi-walled carbon nanotube (MWCNT) dispersion and poly(styrene-co-acrylonitrile)-g-maleic anhydride (SAN-g-MAH) as a compatibilizer on the electrical conductivity, electromagnetic interference shielding effectiveness (EMI SE), and rheological properties of polycarbonate (PC)/poly(acrylonitrile–butadiene–styrene) (ABS)/MWCNT composites were investigated. The morphological results from the scanning and transmission electron microscope images showed that the droplet size of the ABS decreased when the SAN-g-MAH (5 phr) was added to the PC/ABS (80/20) blend. This result suggests that the SAN-g-MAH acts as an effective compatibilizer in the PC/ABS blend. Also, the MWCNT appeared to be located more in the ABS phase (dispersed phase) than in the PC phase (continuous phase). The interfacial tension of the ABS/MWCNT composite was lower than that of the PC–MWCNT composite, and the lower value of interfacial tension of the ABS/MWCNT composite affected the preferred location of the MWCNT in the ABS phase more than in the PC phase. The electrical conductivities and EMI SE of the PC/ABS/MWCNT composite with the compatibilizer were higher than those of the composite without compatibilizer. The complex viscosity of the PC/ABS/MWCNT composite containing the SAN-g-MAH increased with the frequency compared to that of the composite without SAN-g-MAH. This result is possibly due to the increased degree of MWCNT dispersion. The result of rheological properties is consistent with the results of the morphology, electrical conductivity, and EMI SE of the PC/ABS/MWCNT composite.

I.-S. Han · H. G. Yoon
Department of Materials Science and Engineering, Korea University, Anam-dong, Seoul 136-713, Korea

Y. K. Lee · W. N. Kim (✉)
Department of Chemical and Biological Engineering, Korea University, Anam-dong, Seoul 136-713, Korea
e-mail: kimwn@korea.ac.kr

H. S. Lee
Department of Chemical Engineering, Dong-A University, 840, Hadan2-dong, Saha-gu, Busan 604-714, Korea

Introduction

The polycarbonate (PC) and poly(acrylonitrile–butadiene–styrene) (ABS) blend has good mechanical properties, processibility, and heat resistance. For that reason, the PC/ABS blend has been used in automobiles, home appliances, and electronic equipment such as cellular phones, etc. [1–4]. Unfortunately, the electromagnetic emissions produced by electronic devices can interfere with other devices, causing potential problems. For this reason, many researchers have studied conductive polymer composites that show electrical conductivity and electromagnetic interference shielding effectiveness (EMI SE) [5–16].

Recently, carbon nanotube (CNT) has become a very attractive research source because of its advantageous properties including electrical, mechanical, physical, and chemical [11–18]. However, CNT is difficult to use as a reinforcing filler in the polymer composite, because CNTs generally agglomerate like a bundle in the polymer matrix. Therefore, the dispersion of CNTs in the polymer matrix is very important. Chemical functionalizing is one of the

general methods used to improve CNT dispersion in the polymer matrix [19–21]. However, after being modified by acid or other chemical solvents, CNTs might develop a defect on the surface or their length may be shortened. As a result, the electrical, mechanical, and thermal properties of CNT can be destroyed [20].

Recently, to increase the dispersion of the multi-walled carbon nanotube (MWCNT) in the polymer composites, localization of the conductive filler in polymer blends has been studied by many investigators [22–29]. If the conductive filler tends to locate in the dispersed phase, the dispersion of conductive filler would be increased when the polymer blend is formed as a sea-island structure. If the compatibility of the polymer blend is increased by the addition of a compatibilizer, the distribution of the dispersion phase will be more uniform and the dispersion of MWCNT can increase in the composites. Goldel et al. [22] have studied the localization of MWCNT in a PC and poly (styrene-co-acrylonitrile) (SAN) blend. They observed a higher electrical conductivity of the PC/SAN/MWCNT composite compared to PC or SAN composites with the same MWCNT content by melt processing. In our previous studies of poly(propylene carbonate) (PPC)/poly(lactic acid) (PLA)/MWCNT composites, selective localization of the MWCNT in the PPC phase was shown to improve the conductive paths and, therefore, increase the electrical conductivity of the PPC/PLA/MWCNT composites [29]. The above studies of the polymer/polymer/conductive filler composites mostly focus on the electrical conductivity of the composites; therefore, results for the EMI SE are rarely given. The selective localization of the conductive filler was explained by the difference of interfacial tension between the conductive filler and each polymer, which was induced from the difference in polarities and surface tensions.

In this study, we investigated the effect of MWCNT localization on the morphological, electrical, and rheological properties of PC/ABS/MWCNT composites. The effect of SAN-g-maleic anhydride (MAH) as a compatibilizer on the properties of PC/ABS/MWCNT composites has also been studied. The electrical properties of polymer/polymer/MWCNT composites have been studied by other researchers, however, the use of compatibilizer with the polymer/polymer/MWCNT composites is hardly reported. For the electrical properties, the electrical conductivity and EMI SE of the PC/ABS/MWCNT composites were measured using the four-probe method and vector network analyzer, respectively. The morphological and rheological properties of the PC/ABS/MWCNT composites were measured using scanning electron microscopy, transmission electron microscopy, and an advanced rheometric expansion system.

Table 1 Characteristics of polymers and MWCNT used in this study

Materials	M_n^a	M_w^a	T_g (°C)	Diameter (nm)	Length (μm)
Polycarbonate	11000	30000	156	–	–
ABS	26000	82000	105	–	–
MWCNT			–	9–12	10–15

[a] Measured by GPC

Experimental

Materials

PC and ABS which were designated as PC 30010 and XR401, respectively, were supplied by LG Chemical Ltd. (South Korea). SAN-g-MAH was used as a compatibilizer and was supplied by LG Chemical Ltd. MWCNT was synthesized by the chemical vapor-grown method and was supplied by Jeio Ltd. (South Korea). The diameter of MWCNT ranged from 9 to 12 nm with lengths from 10 to 15 μm. The characteristics of the PC, ABS, and MWCNT are shown in Table 1.

Composite preparations

The PC/ABS/MWCNT composites were prepared by melt mixing, and the materials were dried in a vacuum oven at 80 °C before mixing. For melt mixing, a lab-scale twin screw extruder (Bautek Inc., South Korea) was used and the length to diameter screw ratio was 40:1 (11 mm). The extrusion temperature was set at 230 and 280 °C in the feeding and barrel zones, respectively. The blending ratio of PC and ABS was 80/20 (wt%), and the MWCNT contents added in the PC/ABS/MWCNT composite were 1, 3, and 5 parts per hundred parts resin by weight (phr). The SAN-g-MAH was added 5 phr in the PC/ABS blend and PC/ABS/MWCNT composite. For the investigation of electrical and rheological properties, samples were prepared using a hot press at 260 °C and 20 MPa for 3 min.

Morphology

The morphology of the PC/ABS (80/20)/MWCNT composites was investigated using a field emission scanning electron microscope (SEM) (Hitachi S-4300SE, Tokyo, Japan). Samples were cryogenically fractured and coated with white gold before scanning. The accelerating voltage was 25 kV. Images of the microstructure of the PC/ABS/MWCNT composites were taken using a transmission electron microscope (TEM) (FEI Tecnai 20, Eindhoven, Netherlands) with unstained specimens. The sectioning thickness was around 100 nm prepared by the ultramicrotome

technique (Power-Tome PC Ultramicrotome, Boeckeler Instruments, Inc., Arizona, USA) at a general temperature for TEM observation.

Contact angle measurements

Contact angle measurements of the PC and ABS were carried out using the contact angle analyzer (model GonioStar 150, Surfacetech, South Korea). The size of the polymer specimen was 3.0 × 5.0 cm^2 with a 2 mm thickness. Polymer specimens were prepared using hot press. Distilled water was dropped on the surface of the polymer sheet. Then, the measurement of contact angle was made between water drop and polymer sheet. For all measurements, five specimens were measured and averaged.

Rheology

Dynamic measurements of rheological properties were carried out using the advanced rheometric expansion system (ARES model 2 K FRTN 1, USA). Frequency sweeps from 0.1 to 100 rad/s were performed at 260 °C under dry nitrogen conditions. For all measurements, PC/ABS/MWCNT samples were tested within the linear viscoelastic strain range.

Electrical properties

To measure the electrical conductivity, the four-probe method was used to eliminate contact resistance using a digital multimeter (model 2000 multimeter, Keithley). Four thin gold wires (0.05 mm thick and 99 % gold) were attached in parallel to the samples with conducting graphite paint [30]. For electromagnetic interference shielding efficiency (EMI SE) measurements, the PC/ABS/MWCNT composites were connected to a vector network analyzer (Agilent-HP 8719ES-400 Network Analyzer) with a two-ports flanged coaxial line holder. EMI SE was measured in the far-field region for magnetic composite films with a frequency range of 0.05–1.5 GHz using the ASTM D4935-99 method [31]. The reference and load specimens must be the same material and thickness. The diameter and thickness of the specimens were 13.3 cm and 2 mm, respectively. The specimen of the PC/ABS (80/20)/MWCNT composites was obtained using injection molding machine.

Results and discussion

Morphology

Figure 1a–b shows transmission electron micrographs of the PC/ABS (80/20, wt%) blend without and with the compatibilizer of SAN-g-MAH (5 phr), respectively. From Fig. 1, it is observed that the droplet size of the ABS was decreased from 2.61 to 0.46 μm when the SAN-g-MAH (5 phr) was added in the PC/ABS (80/20) blend. This result suggests that the SAN-g-MAH successfully acts as a compatibilizer in the PC/ABS (80/20) blend.

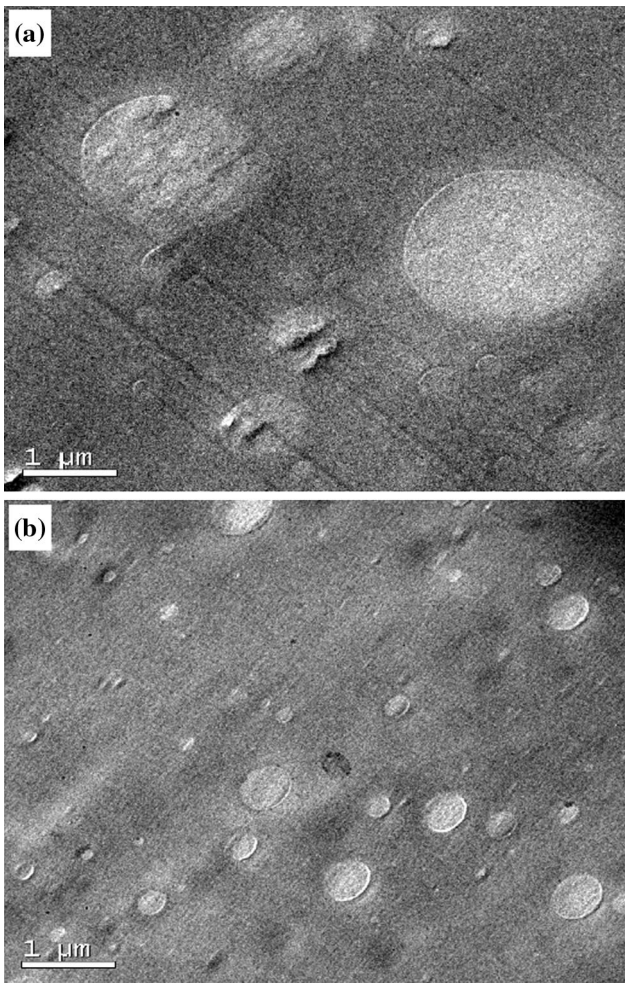

Fig. 1 Transmission electron micrographs of **a** PC/ABS (80/20) blend and **b** PC/ABS (80/20) blend with compatibilizer (SAN-g-MAH, 5 phr)

Figure 2a–b shows the schematic diagram of the PC/ABS/MWCNT composite without and with the compatibilizer, respectively. The domain size of the PC/ABS blend is seen to decrease when the compatibilizer is added. The maleic anhydride (MAH) which contains carbonyl group is highly polar; therefore, the MAH will interact with the polar ester group in PC when they are blended. Also, the ABS contains SAN group, and van der Waals force will exist between the ABS and SAN-g-MAH. Therefore, it is expected that interfacial tension between PC and ABS will be decreased after addition of the SAN-g-MAH in the PC/ABS blend. As a result, the domain size will be decreased when the SAN-g-MAH is added in the PC/ABS blend [32].

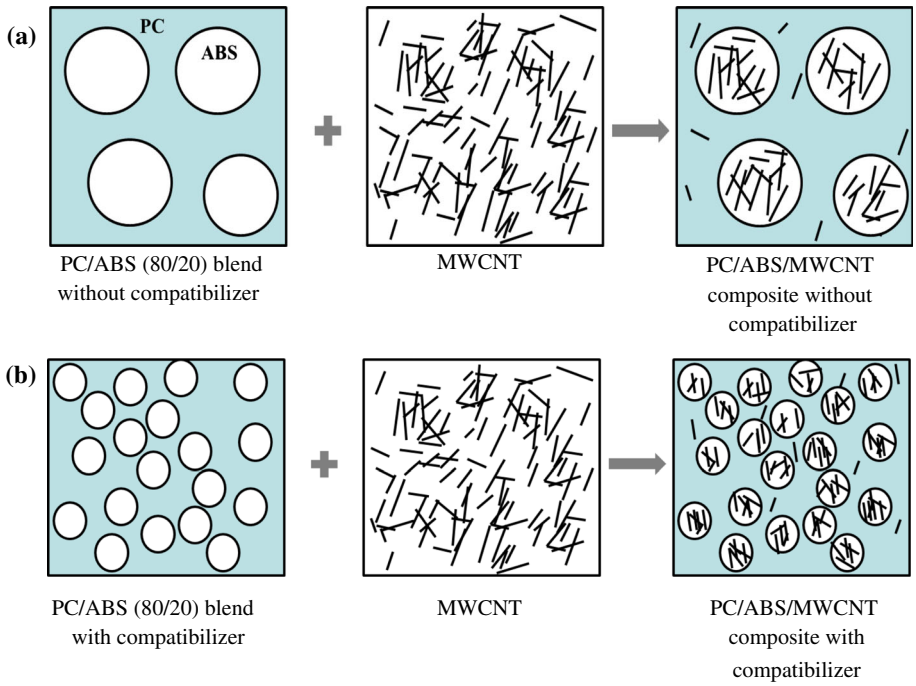

Fig. 2 Schematic diagram of the PC/ABS/MWCNT composites: **a** without compatibilizer; **b** with compatibilizer

Conductive fillers tend to prefer to locate in the phase that has a lower interfacial tension in the polymer/conductive filler composite [29, 33]. From Fig. 2, the MWCNT appears to be located more in the ABS phase (dispersed phase) than in the PC phase which is the continuous phase. After measurements of interfacial tension of the PC/MWCNT and ABS/MWCNT composites and from the results of SEM and TEM analysis of the composites, the schematic diagram of Fig. 2 can be understood more clearly as will be explained later.

Figure 3 shows scanning electron micrographs of the cross-sectional surface of the PC/ABS (80/20)/MWCNT (3 phr) composite with the compatibilizer (SAN-g-MAH, 5 phr) by cryogenically fracturing. The SEM morphology shows that the PC/ABS (80/20) blend is immiscible. Since the morphology of the PC/ABS/MWCNT composite is not clearly shown by SEM, we used TEM to more clearly observe the morphology of the composite. Figure 4a–b shows the transmission electron micrographs of the PC/ABS (80/20)/MWCNT (3 phr) composite without and with the SAN-g-MAH (5 phr), respectively. As observed in Fig. 1, the domain size of Fig. 4b is observed to decrease with the addition of the compatibilizer (SAN-g-MAH, 5 phr). The MWCNT appears to be located more in the ABS phase (dispersed phase) than in the PC phase (dispersed phase). However, some of the MWCNTs are found in the PC phase. The above results of the preferred localization of MWCNT in one phase can be explained by measuring the interfacial tension of the PC/MWCNT and ABS/MWCNT composites, which will be discussed in the following section.

Interfacial tension of MWCNT and polymers

The localization of MWCNT in the PC/ABS (80/20) blend was further examined by measuring the interfacial tension of the PC/MWCNT and ABS/MWCNT composites. The interfacial tension (γ_{12}) can be calculated from the harmonic-mean equation [34], which is a general method for calculating the interfacial tension between two components, as shown in Eq. (1):

$$\gamma_{12} = \gamma_1 + \gamma_2 - 4\left[\frac{\gamma_1^d\gamma_2^d}{\gamma_1^d + \gamma_2^d} + \frac{\gamma_1^p\gamma_2^p}{\gamma_1^p + \gamma_2^p}\right] \quad (1)$$

where γ_1 and γ_2 are the surface tension of the components 1 and 2, respectively, γ^d is the dispersive part of the surface tension, and γ^p is the polar part of the surface tension [34, 35]. The surface tensions of PC, ABS, and MWCNT were 34.5, 36.8, and 45.3 mJ/m^2, respectively (Table 2). The surface tensions of the PC and ABS were obtained from the contact angle measurements (PC = 70.8° and ABS = 65.4°). The surface tension of MWCNT was obtained from Nuriel et al. [36]. The surface tensions for the γ^d and γ^p were calculated from Van Krevelen and Te Nijenhuis [35]. From the surface tensions shown in Table 2, the interfacial tensions of the PC–ABS, PC–MWCNT, and ABS–MWCNT pairs were calculated using Eq. (1), and the results were found to be 8.2, 10.8, and 0.9 mJ/m^2, respectively. From the calculated interfacial tensions between the MWCNT and polymers, it is observed that the interfacial tension of the ABS–MWCNT pair is lower than that of the PC–MWCNT pair.

From the results of TEM analysis of Fig. 4, MWCNTs appear to be more localized in the ABS phase (dispersed

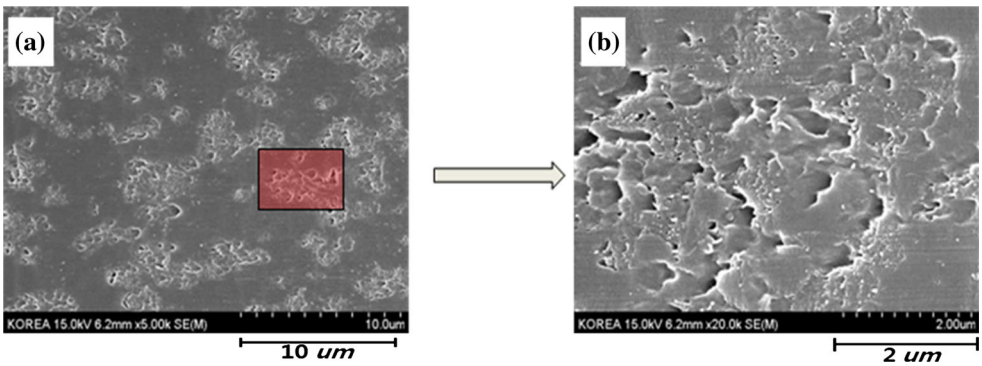

Fig. 3 Scanning electron micrographs of the PC/ABS(80/20)/MWCNT (3 phr) composites with the compatibilizer (SAN-g-MAH, 5 phr): **a** low magnification; **b** high magnification

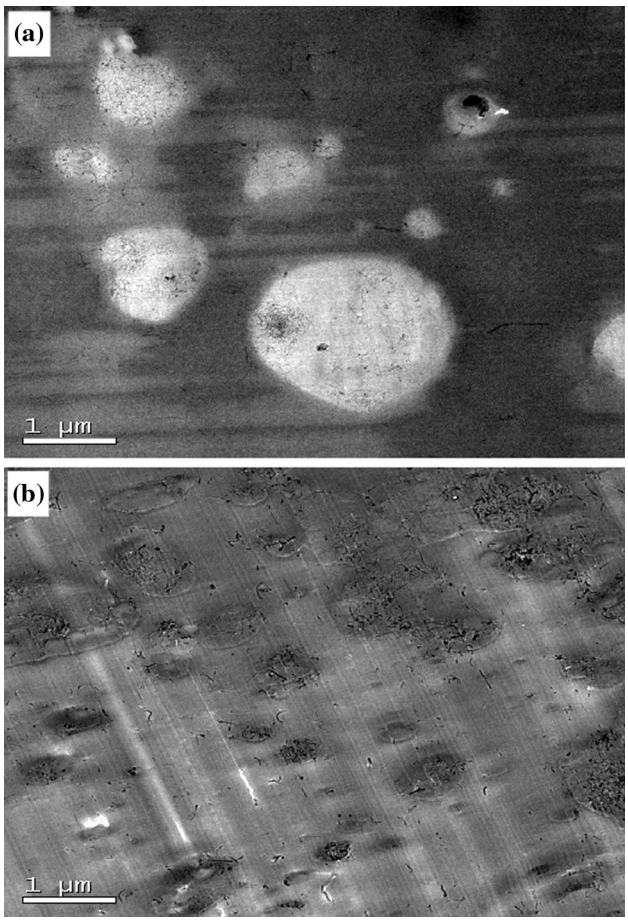

Fig. 4 Transmission electron micrographs of the PC/ABS (80/20)/MWCNT (3 phr) composites: **a** without compatibilizer; **b** with compatibilizer (SAN-g-MAH, 5 phr)

Table 2 Surface tensions (γ) of dispersive part (γ^d) and polar part (γ^p) for polycarbonate, poly(acrylonitrile–butadiene–styrene) (ABS), multi-walled carbon nanotube (MWCNT), and water

Materials	γ (mJ/m^2)	γ^d (mJ/m^2)	γ^p (mJ/m^2)
Polycarbonate	34.5	3.3	31.2
ABS	36.8	14.2	22.6
MWCNT	45.3	18.4	26.9
Water	72.8	21.8	51.0

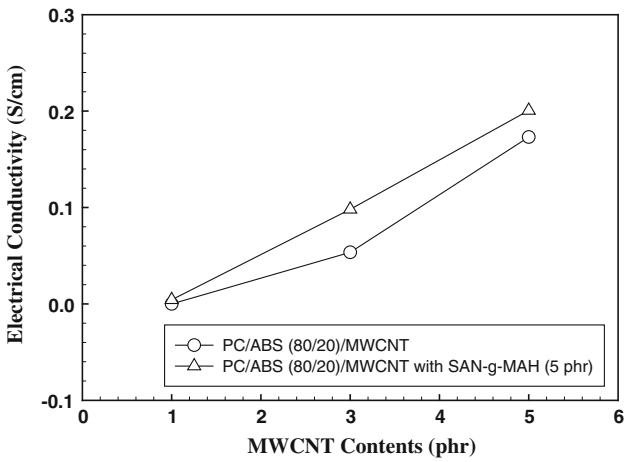

Fig. 5 Electrical conductivity of the PC/ABS(80/20)/MWCNT composites with the MWCNT content: (*open circle*) without compatibilizer; (*open triangle*) with compatibilizer (SAN-g-MAH, 5 phr)

phase) than in the PC phase (continuous phase). Since the interfacial tension of the ABS/MWCNT composite was lower than that of the PC/MWCNT composite, MWCNT tended to locate more in the ABS phase. The melt viscosities of the PC and ABS are similar at the high frequency of about 100 rad/s; therefore, the localization of the MWCNT is dependent on a combination of thermodynamic and kinetic parameters. Since selective localization of MWCNT can result in the formation of a conductive path, the localization of MWCNT may affect the electrical conductivity of the PC/ABS/MWCNT composite [29, 33].

Electrical property of the PC/ABS/MWCNT composites

Figure 5 shows the electrical conductivities (σ) of the composite of PC/ABS (80/20) with the MWCNT content. From the results of Fig. 4, the electrical conductivities of

the PC/ABS/MWCNT composites with and without the compatibilizer (SAN-g-MAH, 5 phr) increased with an increase of the MWCNT content. For the PC/ABS/MWCNT composite with the compatibilizer, the electrical conductivities were found to be 4.3×10^{-3}, 9.8×10^{-2}, and 2.0×10^{-1} S/cm when the MWCNT content was 1, 3, and 5 phr, respectively.

For the PC/ABS/MWCNT composite with the compatibilizer, the electrical conductivities were higher than those of the composite without the compatibilizer. This behavior possibly occurs because the conductive path can be made more easily when the domain size is decreased and, as a result, the MWCNT can be dispersed more evenly. Since the MWCNT presents more in the domain (ABS phase), the electrical conductivity will be increased when the domain size is decreased and when the number of the domain is increased, as we have seen from the TEM results (Fig. 4).

Figure 6 shows the EMI SE of the composite of the PC/ABS (80/20) with the MWCNT (3 wt%) over the frequency range of 0.05–1.5 GHz. The EMI SE is defined in terms of the ratio of the power of the incident electric field and transmitted electric field [37]. The relationship between the electrical conductivity and EMI SE is shown in Eq. (2). From Eq. (2), the EMI SE increases as the electrical conductivity of the composite increases based on the EMI far-field shielding theory [16, 31]:

$$\text{EMI SE} = 20 \log \left(1 + \frac{1}{2}\sigma \, \mathrm{d} Z_0\right) \tag{2}$$

where σ is the electrical conductivity, d the sample thickness, and Z_0 the free space impedance (constant: 377/S).

Figure 6 shows that the EMI SE of the PC/ABS/MWCNT composite increased with the addition of SAN-g-MAH (5 phr) compared to that of the composite without SAN-g-MAH. From Fig. 6, the EMI SE of the PC/ABS/MWCNT composite with the compatibilizer ranged from 5.4 to 8.4 dB, and the composite without the compatibilizer ranged from 2.5 to 4.2 dB at a frequency of 0.1 to 1.5 GHz. From the result shown in Fig. 6, it is suggested that the SAN-g-MAH affected the dispersion of the MWCNT in the composite. Therefore, the increased MWCNT–MWCNT network structure resulted in an increase in the EMI SE when compared with the PC/ABS/MWCNT composite without SAN-g-MAH. From the results of electrical conductivity and EMI SE of the PC/ABS/MWCNT composite, it is suggested that the electrical conductivity and EMI SE are strongly dependent on the degree of MWCNT dispersion in the polymer matrix.

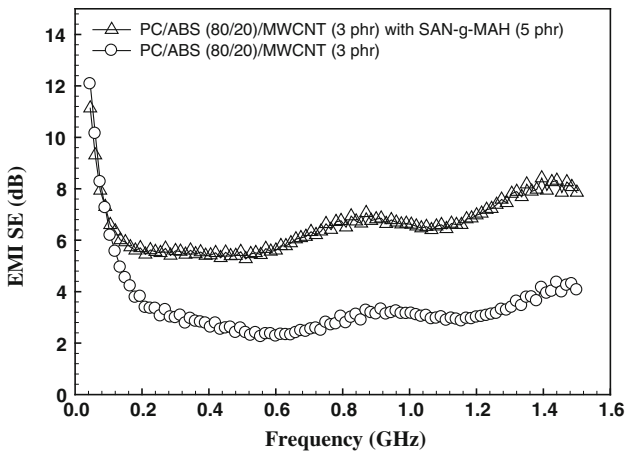

Fig. 6 EMI SE of the PC/ABS(80/20)/MWCNT (3 phr) composites with frequency: (*open circle*) without compatibilizer; (*open triangle*) with compatibilizer (SAN-g-MAH, 5 phr)

Rheological property

Figure 7 shows the complex viscosity (η^*) of the PC, ABS, and PC/ABS (80/20) blend with and without SAN-g-MAH (5 phr). For the PC and ABS, the complex viscosity of the ABS was higher than that of the PC. For the PC/ABS (80/20) blend with and without the SAN-g-MAH, the complex viscosity of the blend decreased with the frequency. The values of the complex viscosity at a frequency of 5.0 rad/s were 1250.8 and 539.7 Pa s for the PC/ABS (80/20) blend with and without SAN-g-MAH, respectively. This result suggests that SAN-g-MAH acts as a compatibilizer between the PC and ABS phases. Therefore, the increase in the viscosity was observed when the compatibilizer was added to the PC/ABS blend. In the studies of the polyamide 6/SAN blend, similar results were reported by Jafari et al. [38].

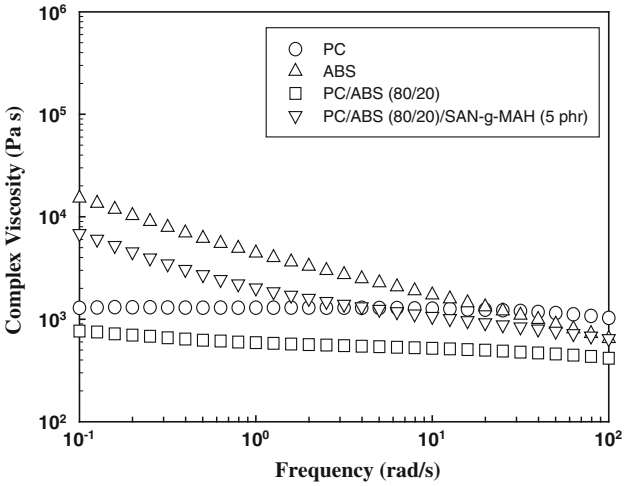

Fig. 7 Complex viscosity of the PC/ABS blend with frequency: (*open circle*) PC; (*open triangle*) ABS; (*open square*) PC/ABS (80/20); (*open down pointing triangle*) PC/ABS (80/20) with SAN-g-MAH (5 phr)

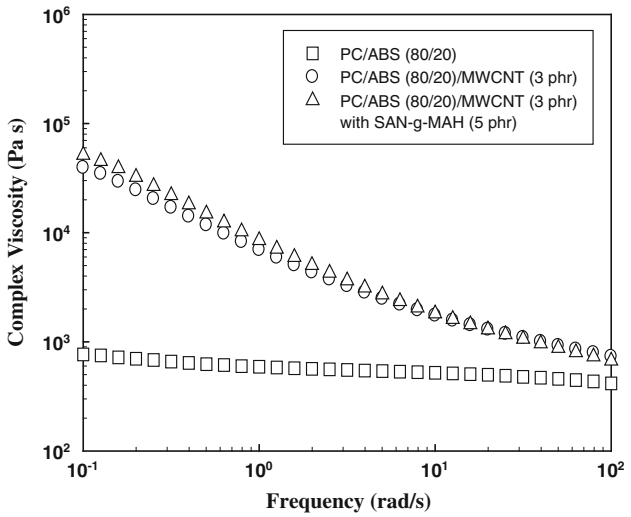

Fig. 8 Complex viscosity of the PC/ABS blend and PC/ABS/MWCNT composites with frequency: (*open square*) PC/ABS (80/20); (*open circle*) PC/ABS (80/20)/MWCNT (3 phr); (*open triangle*) PC/ABS (80/20)/MWCNT (3 phr) with SAN-g-MAH (5 phr)

Figure 8 shows the complex viscosity of the PC/ABS (80/20)/MWCNT (3 phr) composites with and without SAN-g-MAH (5 phr). For the PC/ABS/MWCNT composite with and without the SAN-g-MAH, the complex viscosity of the composite decreased with the frequency. For the PC/ABS/MWCNT composite at a frequency of 5.0 rad/s, the values of the complex viscosity were 2703.2 and 2482.6 Pa s with and without SAN-g-MAH, respectively. The increase in complex viscosity of the composites with the SAN-g-MAH was more significant at the low frequencies than at high frequencies. The rheological properties of the polymer composites at low frequencies reflect the dispersion of the filler [12, 18, 39].

In the studies of single-walled carbon nanotube and poly(methyl methacrylate) composite, Du et al. [18] reported that the higher values of the complex viscosity were associated with better nanodispersion of the carbon nanotube, when all other factors were constant. In our early studies of PPC/MWCNT composite, similar results showed that higher MWCNT dispersion resulted in an increased complex viscosity of the composite [29]. Therefore, from the results shown in Fig. 8, the increased complex viscosity of the PC/ABS/MWCNT composite with the SAN-g-MAH was possibly due to the increased degree of MWCNT dispersion. This result is consistent with the results of electrical conductivity and EMI SE of the PC/ABS/MWCNT composite.

Conclusions

In this study, the morphological, electrical, and rheological properties of the PC/ABS (80/20)/MWCNT composite with the SAN-g-MAH as a compatibilizer were investigated. From the results of morphological studies by SEM and TEM, the droplet size of the ABS was decreased from 2.61 to 0.46 μm when the SAN-g-MAH (5 phr) was added to the PC/ABS blend, which suggested that the SAN-g-MAH successfully acted as a compatibilizer in the PC/ABS blend. Also, the MWCNT appeared to be located more in the ABS phase (dispersed phase) than in the PC phase (continuous phase). From the measurements of interfacial tension of the composites, the interfacial tension of the ABS/MWCNT composite was lower than that of the PC–MWCNT composite. From this result, it was suggested that the lower value of interfacial tension of the ABS/MWCNT composite affected the preferred location of the MWCNT in the ABS phase more than in the PC phase.

The electrical conductivities and EMI SE of the PC/ABS/MWCNT composite with the compatibilizer were higher than that of the composite without compatibilizer. This behavior is possibly due to the increased MWCNT dispersion when the domain size (ABS phase) is decreased and when the number of domains is increased. When the domain size is decreased, the MWCNT–MWCNT network is increased. Therefore, the electrical conductivities and EMI SE of the PC/ABS/MWCNT composite were increased.

For the PC/ABS/MWCNT composite with the SAN-g-MAH, the complex viscosity of the composite increased with the frequency compared to that of the composite without SAN-g-MAH. The increased complex viscosity of the PC/ABS/MWCNT composite with the SAN-g-MAH was possibly due to the increased degree of MWCNT dispersion. The storage modulus of polymer composites at low frequencies reflects the dispersion of the filler. The result of rheological properties is consistent with the results of the morphology, electrical conductivity, and EMI SE of the PC/ABS/MWCNT composite.

Acknowledgements This work (Grants No. C0102544) was supported by the Business for Cooperative R&D between Industry, Academy, and Research Institute funded by the Korea Small and Medium Business Administration in 2013.

References

1. Suarez H, Barlow JW, Paul DR (1984) Mechanical properties of ABS/polycarbonate blends. J Appl Polym Sci 29:3253
2. Kim WN, Burns CM (1988) Thermal behavior, morphology, and some melt properties of blends of polycarbonate with poly(styrene-co-acrylonitrile) and poly(acrylonitrile–butadiene–styrene). Polym Eng Sci 28:1115
3. Chun JH, Maeng KS, Suh KS (1991) Miscibility and synergistic effect of impact strength in polycarbonate/ABS blends. J Mater Sci 26:5347
4. Tjong SC, Meng YZ (2000) Effect of reactive compatibilizers on the mechanical properties of polycarbonate/poly(acrylonitrile–butadiene–styrene) blends. Eur Polym J 36:123

5. Han MS, Lee YK, Lee HS, Yun YH, Kim WN (2009) Electrical, morphological and rheological properties of carbon nanotube composites with polyethylene and poly(phenylene sulfide) by melt mixing. Chem Eng Sci 64:4649
6. You KM, Park SS, Lee CS, Kim JM, Park GP, Kim WN (2011) Preparation and characterization of conductive carbon nanotube-polyurethane foam composites. J Mater Sci 46:6850. doi:10.1007/s10853-011-5645-y
7. Rahaman M, Chaki TK, Khastgir D (2011) Development of high performance EMI shielding material from EVA, NBR, and their blends: effect of carbon black structure. J Mater Sci 46:3989. doi:10.1007/s10853-011-5326-x
8. Sachdev VK, Patel K, Bhattacharya S, Tandon RP (2011) Electromagnetic interference shielding of graphite/acrylonitrile butadiene styrene composites. J Appl Polym Sci 120:1100
9. Zhang L, Wang LB, See KY, Ma J (2013) Effect of carbonfiber reinforcement on electromagnetic interference shielding effectiveness of syntactic foam. J Mater Sci 48:7757. doi:10.1007/s10853-013-7597-x
10. Huang CY, Wu CC (2000) The EMI shielding effectiveness of PC/ABS/nickel-coated-carbon-fibre composites. Eur Polym J 36:2729
11. Im JS, Kim JG, Lee YS (2009) Fluorination effects of carbon black additives for electrical properties and EMI shielding efficiency by improved dispersion and adhesion. Carbon 47:2640
12. Sung YT, Han MS, Song KH, Jung JW, Lee HS, Kum CK, Joo J, Kim WN (2006) Rheological and electrical properties of polycarbonate/multi-walled carbon nanotube composites. Polymer 47:4434
13. Papanicolaou GC, Papaefthymiou KP, Koutsomitopoulou AF, Portan DV, Zaoutsos SP (2012) Effect of dispersion of MWCNTs on the static and dynamic mechanical behavior of epoxy matrix nanocomposites. J Mater Sci 47:350. doi:10.1007/s10853-011-5804-1
14. Imran SM, Kim Y, Shao GN, Hussain M, Choa YH, Kim HT (2014) Enhancement of electroconductivity of polyaniline/grapheme oxide nanocomposites through in situ emulsion polymerization. J Mater Sci 49:1328. doi:10.1007/s10853-013-7816-5
15. Zetina-Hernandez O, Duarte-Aranda S, May-Pat A, Canche-Escamilla G, Uribe-Calderon J, Gonzalez-Chi P, Aviles F (2013) Coupled electro-mechanical properties of multiwall carbon nanotube/polypropylene composites for strain sensing applications. J Mater Sci 48:7587. doi:10.1007/s10853-013-7575-3
16. Yoo TW, Lee YK, Lim SJ, Yoon HG, Kim WN (2014) Effects of hybrid fillers on the electromagnetic interference shielding effectiveness of polyamide 6/conductive filler composites. J Mater Sci 49:1701. doi:10.1007/s10853-013-7855-y
17. Lee DW, Ma S, Lee KY (2013) Electrical and mechanical properties of carbon/glass hybridized long fiber reinforced polypropylene composites. Macromol Res 21:767
18. Du F, Scogna RC, Zhou W, Brand S, Fischer JE, Winey KI (2004) Nanotube networks in polymer nanocomposites: rheology and electrical conductivity. Macromolecules 37:9048
19. Yan H, Kou K (2014) Enhanced thermoelectric properties in polyaniline composites with polyaniline-coated carbon nanotubes. J Mater Sci 49:1222. doi:10.1007/s1085-013-7804-9
20. Li QF, Xu Y, Yoon JS, Chen GX (2011) Dispersions of carbon nanotubes/polyhedral oligomeric silsesquioxanes hybrids in polymer: the mechanical, electrical and EMI shielding properties. J Mater Sci 46:2324. doi:10.1007/s10853-010-5077-0
21. Zheng J, Zhu Z, Qi J, Zhou Z, Li P, Peng M (2011) Preparation of isotactic polypropylene-grafted multiwalled carbon nanotubes (iPP-g-MWCNTs) by macroradical addition in solution and the properties of iPP-g-MWCNTs/iPP composites. J Mater Sci 46:648
22. Goldel A, Kasaliwal G, Potschke P (2009) Selective localization and migration of multiwalled carbon nanotubes in blends of polycarbonate and poly(styrene–acrylonitrile). Macromol Rapid Commun 30:423
23. Zou H, Wang K, Zhang Q, Fu Q (2006) A change of phase morphology in poly(p-phenylene sulfide)/polyamide 66 blends induced by adding multi-walled carbon nanotubes. Polymer 47:7821
24. Wu D, Zhang Y, Zhang M, Yu W (2009) Selective localization of multiwalled carbon nanotubes in polycaprolactone/polylactide blend. Biomacromolecules 10:417
25. Dai K, Xu XB, Li ZM (2007) Electrically conductive carbon black (CB) filled in situ microfibrillar poly(ethylene terephthalate) (PET)/polyethylene (PE) composite with a selective CB distribution. Polymer 48:849
26. Potschke P, Pegel S, Claes M, Bonduel D (2008) A novel strategy to incorporate carbon nanotubes into thermoplastic matrices. Macromol Rapid Commun 29:244
27. Bose S, Bhattacharyya AR, Kulkarni AR, Potschke P (2009) Multiwall carbon nanotubes prepared by melt blending. Compos Sci Tech 69:365
28. Ko SW, Hong MK, Park BJ, Gupta RK, Choi HJ, Bhattaxharya SN (2009) Morphological and rheological characterization of multi-walled carbon nanotube/PLA/PBAT blend nanocomposites. Polym Bull 63:125
29. Park DH, Kan TG, Lee YK, Kim WN (2013) Effect of multi-walled carbon nanotube dispersion on the electrical and rheological properties of poly(propylene carbonate)/poly(lactic acid)/multi-walled carbon nanotube composites. J Mater Sci 48:481. doi:10.1007/s10853-012-6762-y
30. Joo J, Lee CY (2000) High frequency electromagnetic interference shielding response of mixtures and multilayer films based on conducting polymers. J Appl Phys 88:513
31. Colaneri NF, Shacklette LW (1992) EMI shielding measurements of conductive polymer blends. IEEE Trans Instrum Meas 41:291
32. Lee JB, Lee YK, Choi GD, Na SW, Park TS, Kim WN (2011) Compatibilizing effects for improving mechanical properties of biodegradable poly(lactic acid) and polycarbonate blends. Polym Degrad Stab 96:553
33. Sumita M, Sakata K, Asai S, Miyasaka K, Nakagawa H (1991) Dispersion of fillers and the electrical conductivity of polymer blends filled with carbon black. Polym Bull 25:265
34. Wu S (1982) Polymer interface and adhesion. Marcel Dekker, New York
35. Van Krevelen DW, Te Nijenhuis K (2009) Properties of polymers. Elsevier, Amsterdam
36. Nuriel S, Liu L, Barber AH, Wagner HD (2005) Direct measurement of multiwall nanotube surface tension. Chem Phys Lett 404:263
37. White DRJ (1971) EMI/EMC handbook series 4. Don White Consultants, Warrenton
38. Jafari SH, Potschke P, Stephan M, Warth H, Alberts H (2002) Multicomponent blends based on polyamide and styrenic polymers: morphology and melt rheology. Polymer 43:6985
39. Mitchell CA, Bahr JL, Arepalli S, Tour JM, Krishnamoorti R (2002) Dispersion of functionalized carbon nanotubes in polystyrene. Macromolecules 35:8825